



UNIVERSIDAD DE SONORA

DIVISIÓN DE CIENCIAS EXACTAS Y NATURALES
DEPARTAMENTO DE INVESTIGACIÓN EN FÍSICA

MEASUREMENTS OF THE LARGE HADRON COLLIDER LUMINOSITY USING THE CMS SILICON PIXEL DETECTOR

THESIS

in partial fulfillment of the requirements for the degree of:

Maestría en Ciencias (Física)

By:

Luis Enrique CUEVAS PICOS

Director:

Dr. Jose Feliciano BENITEZ RUBIO

Hermosillo, Sonora

May, 2023

Acknowledgements

I would like to thank my wife Elizabeth for her unconditional support in the challenges I set myself, without her this would not be possible. To my advisor, Dr. José Benítez, for giving me guidance, patience and, above all, the opportunity to work in such a professional team and join the CMS experiment, that was a dream for me. To the University of Sonora and CONACYT for supporting me in completing this important challenge in my professional career.

Abstract

The calibration of the luminosity measurement from the analysis of the van der Meer scanning program for the CMS experiment in the 2022 proton-proton collision data-taking at $\sqrt{s}=13.6$ TeV with the CMS Silicon Pixel detector is described. The data collection period was on November 11 for the LHC fill 8381, the recorded data collected was reprocessed along with a selection of good modules based on luminosity stability studies. The Analysis of the van der Meer scans with some especific corrections present results in the calibration constant $\sigma_{vis} = 4163 \pm 3(\text{stat.}) \pm 12(\text{syst.})$ mb.

Resumen

Table of contents

List of figures	vi
List of tables	vii
1 Introduction	1
1.1 Fundamental Particles	1
1.2 Particle Colliders	3
1.3 Cross section	5
1.4 Luminosity	7
1.5 Importance of Luminosity precision	10
1.6 The Large Hadron Collider	11
1.7 LHC Luminosity	13
2 Experiment Description	15
2.1 The Compact Muon Solenoid	15
2.2 CMS Tracking System	15
2.2.1 Pixel Detector and Clustering	15
2.2.2 CMS Luminometers	15
3 Luminosity Measurement and Calibration	16
3.1 Luminosity calibration: van der Meer method	16
4 Analysis and Results	17
4.1 2018 vdM scan program	17
4.2 Data analysis	17
4.3 Module selection	17
4.4 Background estimation	17
4.5 Corrections	17
5 Summary and Outlook	18
References	19

List of figures

1.1	Cross section illustration	6
1.2	Colliding beam interaction	8
1.3	LHC Complex	12
1.4	CMS Luminosity per year	13

List of tables

1.1	The twelve fundamental fermions divided into quarks and leptons. The masses of the quarks are the current masses.	2
1.2	Force experienced by the fermions	2

Chapter 1

Introduction

Particle physics is the study of fundamental particles and forces that constitute matter and radiation of the universe. The fundamental particles and the interaction between them are classified in the Standard Model as fermions (matter particles) and bosons (force-carrying particles). The study of these interactions is carried out using high-energy particle accelerators, which measure a large number of parameters and properties of the particles produced at the time of the collisions .

This chapter gives a brief background of the elementary particles, particle colliders and the measure of the performance of these, emphasizing the concepts and definitions necessary for the understanding of this thesis project.

1.1 Fundamental Particles

The universe is constituted from a few different particles. Atoms are the bound states of negatively charged electrons (e^-) which orbit around a central nucleus composed of positively charged protons (p) and electrically neutral neutrons (n). The electrons are bound to the nucleus by the electrostatic attraction between opposite charges, The protons and neutrons are bound together by the strong nuclear force. The fundamental interactions of particle physics are completed by the weak force and gravity , the first is responsible for the nuclear -decays and the nuclear fusion, the second which although extremely weak, is always attractive and is therefore responsible for large-scale structure in the Universe.

This is a very simple physical model, but at higher energy scales, more structure is observed, and this is where our current understanding leads us to the existence of 17 fundamental particles that constitute our entire universe, these are divided into two groups:

fermions with spin $1/2$, and bosons with integer spin [1].

The fermions are the particles that constitute the matter, there are a total of twelve of these fundamental particles and they are classified into two types, leptons and quarks, which in turn are divided into three generations (first, second and third), each member of a higher generation has a greater mass than the corresponding particle of the previous generation; There are six leptons, three charged: electron (e), muon (μ) and tau (τ), and their corresponding neutrinos: electron-neutrino (ν_e), muon - neutrino (ν_μ) and tau-neutrino (ν_τ). The other group of fermions are quarks, these can only be found coupled to form particles called hadrons. The group of quarks is formed by the up quark (u), the down quark (d), the charm quark (c), the strange quark (s), the top quark (t) and the bottom quark (b)[2]. The properties of these twelve particles are shown in table 1.1

Table 1.1 The twelve fundamental fermions divided into quarks and leptons. The masses of the quarks are the current masses.

Leptons					Quarks		
	Particle		Q	mass/GeV	Particle	Q	mass/GeV
First generation	electron (e^-)		-1	0.0005	down (d)	-1/3	0.003
	neutrino (ν_e)		0	$<10^{-9}$	up (u)	+2/3	0.005
Second generation	muon (μ^-)		-1	0.106	strange (s)	-1/3	0.1
	neutrino (ν_μ)		0	$<10^{-9}$	charm (c)	+2/3	1.3
Third generation	tau (τ^-)		-1	1.78	bottom (b)	-1/3	4.5
	neutrino (ν_τ)		0	$<10^{-9}$	top (t)	+2/3	174

Bosons describe the interactions between the fermions, these interactions are described by the exchange of particles, which consist of the gauge bosons: photon, W^\pm and Z^0 , and gluons (g , eight of them), respectively. Apart from these vector bosons, there is a special scalar boson called Higgs boson, associated with the mechanism that give mass to all fundamental particles. The force experienced by the fermions is shown in table. 1.2.

Table 1.2 Force experienced by the fermions

				Electromagnetic	Weak	Strong
Leptons	e	μ	τ	✓	✓	
	ν_e	ν_μ	ν_τ			
Quarks	u	c	t	✓	✓	✓
	d	s	b			

All these particles are described by the Standard Model (SM), the best theoretical model that provides a successful description of the experimental data. Most of this data comes from particle colliders because they can only be produced and studied using collisions of high energy.

1.2 Particle Colliders

Most of the recent breakthroughs in particle physics have come from experiments at high-energy particle accelerators, they are the most powerful microscopes for viewing the tiniest inner structure of cells, genes, molecules, atoms and their constituent protons, neutrons, electrons, neutrinos, quarks, and possible still undiscovered even more fundamental building blocks of the universe such as dark matter and dark energy.

Particle Colliders produce and accelerate beams of charged particles at high speeds, close to the speed of light, using electromagnetic fields ; the high-energy collisions of these beams produce individual interactions referred to as events. These collisions produce massive particles, such as the Higgs boson or the top quark. These particles only last in the blink of an eye, and cannot be observed directly, almost immediately they transform (or decay) into lighter particles, which in turn also decay. They are measured and identified by a wide range of experiments (particle detectors), whose technologies, techniques and designs are based on the properties of the particles and on the nature of their interactions with matter.

In general, a detector consists of a cylindrical (or polygonal) barrel part, with its axis parallel to the incoming colliding beams. The cylindrical structure is closed by two flat end caps, providing almost complete solid angle coverage down to the beam pipe. The inner region of the detector is devoted to the tracking of charged particles, the tracking volume is surrounded by an electromagnetic calorimeter for detecting electrons and photons who appear as isolated energy deposits and charged-particle tracks respectively. The relatively large-volume hadronic calorimeter for detecting and measuring the energies of hadrons is located outside the electromagnetic calorimeter. Dedicated detectors are positioned at the outside of the experiment to record the signals from any high-energy muons produced in the collisions, which are the only particles (apart from neutrinos) that can penetrate through the hadronic calorimeter, muons can be identified as charged-particle tracks associated with small energy depositions in both the and signals in the muon detectors on the outside of the detector system. Whilst neutrinos leave no signals in the detector, their presence

often can be inferred from the presence of missing momentum.

The performance of particle colliders is usually quantified by the beam energy and the luminosity, the energy available for the production of new effects is the one of the most important parameter. The required large centre of mass energy which determines the types of particles that can be studied or discovered can only be provided with colliding beams experiments. In these kind of experiments the incident particles are accelerated and the two beams are brought together at an intersection point where they collide into each other, the total energy of a projectile particle plus the target particle depends on the reference frame.

Colliding beam machines have the advantage that they can achieve much higher centre-of-mass energies, at various points the beams intersect and scattering takes place. If the (equal mass) incident particles have the same energy and therefore equal but opposite momentum, then the experiment is taking place in the centre-of-mass (CM) frame and the full energy delivered by the accelerator, can be used to produce high mass particles.

Consider the Lorentz invariant quantity s used in particle physics to denote the square of the total incoming energy in the CM frame:

$$s = \left(\sum_{i=1,2} E_i \right)^2 - \left(\sum_{i=1,2} p_i \right)^2 c^2 \quad (1.1)$$

Where E and p are the energy and the momenta of each incoming particle respectively, in this frame, where the momenta are equal and opposite, the second term vanishes and:

$$s = 4E^2 \quad (1.2)$$

The second important parameter of the collider's performance is the luminosity, defined as the quantity that measures the ability of a particle accelerator to produce the required number of interactions and is the proportionality factor between the number of events per second dR/dt and the quantum mechanical probability for the interaction called cross section σ_p .

1.3 Cross section

The technical meaning of the “cross section” is very different from the common usage. Normally, “cross section” refers to a slice of an object. In particle physics might use the word this way, but more often it is used to mean the probability that two particles will collide and react in a certain way. When proton beams cross in a particle scelerators, many different processes can occur. The cross section of a particular process depends on the type and energy of the colliding particles. At the LHC, certain particles such as W and Z bosons have large cross sections σ_p , so they will be observed more often and the production of a Higgs boson has a much lower cross section σ_p , so is more difficult to produce.

In the simplest case one can imagine a beam of particles of type a , with flux ϕ_a , is crossing a region of space in which there are n_b particles per unit volume of type b . The interaction rate per target particle r_b will be proportional to the incident particle flux, and can be written [1]:

$$r_b = \sigma \phi_a$$

The fundamental physics is contained in σ , which has dimensions of area, and is termed as interaction cross section. Sometimes it is helpful to think of σ as the effective cross sectional area associated with each target particle. Indeed, There are cases where the cross section is closely related to the physical cross sectional area of the target, for example, neutron absorption by a nucleus. However, in general, the cross section is simply an expression of the underlying quantum mechanical probability that an interaction will occur. [1].

The definition of the cross section is illustrated in Figure 1.1(a), where a single incident particle of type a is travelling with a velocity v_a in a region defined by the area A , which contains n_b particles of type b per unit volume moving with a velocity v_b in the opposite direction to v_a . In time δt , the particle a crosses a region containing $\delta N = n_b(v_a + v_b)A\delta t$ of type b . The interaction probability can be obtained from the *effective* total cross sectional area of the δN particles divided by the area A , which can be thought of as the probability that the incident particle passes through one of the regions of area σ drawn around each of the δN target particles, as shown in Fig. 1.1(b) [1]. The interaction probability δP is therefore

$$\delta P = \frac{\delta N \sigma}{A} = \frac{n_b(v_a + v_b)A\sigma t}{A} = n_b v \sigma \delta t, \quad (1.3)$$

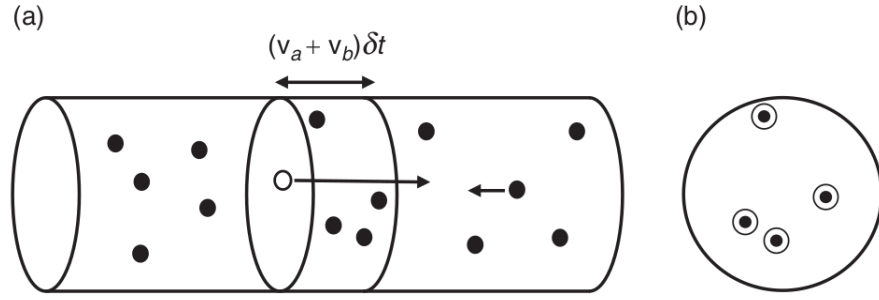


Fig. 1.1 Left hand (a): single incident particle of type a traversing a region containing particles of type b . Right-hand plot (b): projected view of the region traversed by the incident particle in time δt [1].

where $v = v_a + v_b$. The interaction rate for each particle of type a is

$$r_a = \frac{dP}{dt} = n_b v \sigma \quad (1.4)$$

For a beam of particles of type a with number density n_a confined to a volume V , the total interaction rate is

$$\text{rate} = r_a n_a V = (n_b v \sigma) n_a V = (n_a v) (n_b V) \sigma$$

$$\text{rate} = (n_a v) (n_b V) \sigma = \phi N_b \sigma$$

Thus the total rate is equal to

$$\text{rate} = \text{flux} \times \text{number of target particles} \times \text{cross section} \quad (1.5)$$

More formally, the cross section for a process is defined as

$$\sigma = \frac{\text{number of interaction per unit time per target particle}}{\text{incident flux}} \quad (1.6)$$

Where the flux ϕ accounts for the relative motion of particles. One approach to calculate the cross section for a particular process can be using the relativistic formulation of Fermi's golden rule and the appropriate Lorentz-invariant expression for the particle flux.

The cross section for the production of a general final state O at the LHC is given by [3]:

$$\sigma(pp \rightarrow O + X) = \int dx_1 dx_2 \sum_{i,j} f_i(x_1, Q) f_j(x_2, Q) \hat{\sigma}(ij \rightarrow O)(M_O, g_{ijO}, \dots) \quad (1.7)$$

where $f_i(x, Q)$ is the density of partons¹ (PDF) of type i (quarks of different flavours or gluons) inside the proton, carrying a fraction x of the proton momentum at a resolution scale Q . Theory predicts the PDFs to be independent of O . $\hat{\sigma}(ij \rightarrow O)$ is the partonic cross section to produce the final state O in the collisions of partons i and j . It depends on properties of the final state (for example the mass of O , M_O , the momentum of the various particles involved, etc.), and on the nature of the interactions involved in the process (for example the strength, g_{ijO} , of the coupling between i , j and O). Parameters like M_O and g_{ijO} are therefore what defines the underlying theory, and extracting their value as accurately as possible is the ultimate goal of an experimental measurement [3].

1.4 Luminosity

In particle physics experiments the energy available for the production of new effects is the most important parameter. Besides the energy the number of useful interactions (events), is important. The quantity that measures the ability of a particle accelerator to produce the required number of interactions is called the luminosity \mathcal{L}_{inst} and is the proportionality factor between the number of events per second dR/dt and the cross section σ_p [4]:

$$\frac{dR}{dt} = \mathcal{L}_{inst} \cdot \sigma_p \quad (1.8)$$

The unit of luminosity is $cm^{-2}s^{-1}$.

To derive a general expression of luminosity, In the case of two colliding beams, both beams serve as target and "incoming" beam at the same time. We treat the case of bunched beams.

A schematic picture is shown in Fig. 1.2 Since the two beams are not stationary but moving through each other, the overlap integral depends on the longitudinal position of the

¹Before quarks and gluons were generally accepted, Feynman proposed that the proton was made up of point-like constituents, termed partons [1].

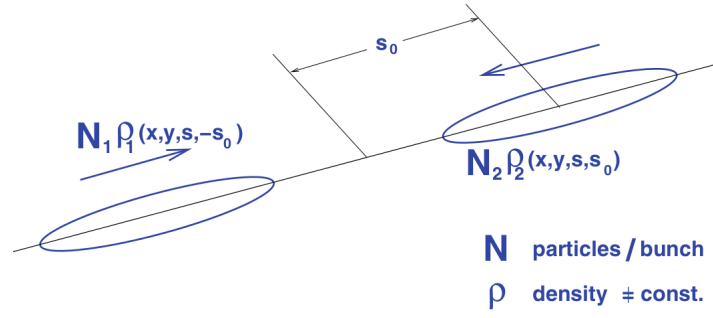


Fig. 1.2 Schematic view of a colliding beam interaction[1].

bunches and therefore on the time as they move towards and through each other, the two beams have different distribution functions and different number of particles in the beams, the overlap integral which is proportional to the luminosity (\mathcal{L}_{inst}) we can then write as:

$$\mathcal{L}_{inst} \propto K \cdot \int \int \int_{-\infty}^{\infty} \rho_1(x, y, s, -s_0) \rho_2(x, y, s, s_0) dx dy ds ds_0 \quad (1.9)$$

Where $\rho_1(x, y, s, -s_0)$ and $\rho_2(x, y, s, s_0)$ are the time dependent beam density distribution functions. We assume, that the two bunches meet at $s_0 = 0$. Because the beams are moving against each other, we have to multiply this expression with a kinematic factor:

$$K = \sqrt{(\vec{v}_1 - \vec{v}_2)^2 - (\vec{v}_1 \times \vec{v}_2)^2 / c^2} \quad (1.10)$$

Assuming head-on collisions ($\vec{v}_1 = -\vec{v}_2$) and that all densities are uncorrelated in all planes. In that case we can factorize the density distributions and get for the overlap integral:

$$\mathcal{L}_{inst} = 2N_b N_1 N_2 f \int \int \int \int_{-\infty}^{\infty} \rho_{1x}(x) \rho_{1y}(y) \rho_{1s}(s - s_0) \rho_{2x}(x) \rho_{2y}(y) \rho_{2s}(s + s_0) dx dy ds ds_0 \quad (1.11)$$

where N_1 and N_2 are the particles per bunch, f the revolution frequency and N_b is the number of bunches in one beam.

Assuming Gaussian profiles in all dimensions of the form:

$$\rho_{iz}(z) = \frac{1}{\sqrt{2\pi}\sigma_z} \exp\left(-\frac{z^2}{2\sigma_z^2}\right) \quad z = x, y \quad i = 1, 2 \quad (1.12)$$

$$\rho_s(s \pm s_0) = \frac{1}{\sqrt{2\pi}\sigma_s} \exp\left(-\frac{(s \pm s_0)^2}{2\sigma_s^2}\right) \quad (1.13)$$

In the case of exactly head-on collisions of bunches travelling almost at the speed of light, the kinematic factor becomes 2, assuming approximately equal bunch lengths $\sigma_{1s} \approx \sigma_{2s}$. Solving eq. 1.11:

For a general case where $\sigma_{1x} \neq \sigma_{2x}$ and $\sigma_{1y} \neq \sigma_{2y}$:

$$\mathcal{L}_{inst} = \frac{N_1 N_2 N_b f}{2\pi \sqrt{\sigma_{1x}^2 + \sigma_{2x}^2} \sqrt{\sigma_{1y}^2 + \sigma_{2y}^2}} \quad (1.14)$$

For a specific case, assuming equal beams, $\sigma_{1x} = \sigma_{2x}$, $\sigma_{1y} = \sigma_{2y}$ and $\sigma_{1s} = \sigma_{2s}$:

$$\mathcal{L}_{inst} = \frac{N_1 N_2 N_b f}{4\pi \sigma_x \sigma_y} \quad (1.15)$$

This is the well known expression for the luminosity of two Gaussian beams colliding head-on. It shows how the luminosity depends on the number of particles per bunch and the beam sizes. This reflects the 2-dimensional target charge density we have seen in the evaluation of the fixed target luminosity.

In practice, the integral in 1.11 cannot be solved analytically because the properties of the colliding beams are not known precisely, so an experimental technique is implemented with a dedicated machine setup to estimate the integrals, yielding a similar expression as 1.15.

The instantaneous luminosity and therefore the maximum luminosity measure is very important because it reflects the performance of the collider, but this is not the only measurement concerned with luminosity. Another important measurement and in the final figure of merit of luminosity is the so-called integrated luminosity [4]:

$$\mathcal{L}_{int} = \int_0^T \mathcal{L}_{inst}(t') dt' \quad (1.16)$$

because it directly relates to the number of observed events:

$$\mathcal{L}_{int} / \text{ndot} / \sigma_p = \text{number of events of interest} \quad (1.17)$$

The integral is taken over a period of time T (excluding possible dead time). The integrated luminosity has units of cm^{-2} and is often expressed in inverse barn ($1barn = 10^{-24}cm^2$).

Another important parameter for a beam with high luminosity and bunched beams are the number of collisions per bunch crossing, the so-called pile up (μ). Pileup and luminosity are related by $f\mu = \mathcal{L}_{inst}\sigma_p$. In particular for collisions with a large cross section this can become a problem. In the case of the LHC The challenge is to maximise the useful luminosity while keeping the pile up to a level that can be handled by the particle detectors.[4]:

1.5 Importance of Luminosity precision

For physics analyses such as searches for new particles, rare processes or measurements of the properties of known particle, it is important not only for accelerators to increase luminosity, but also for physicists to understand it with the best possible precision.

Luminosity is one of the fundamental parameters to measure an accelerator's performance. when two such bunches pass through each other, only a few protons from each bunch end up interacting with the protons circulating in the opposite direction. Luminosity is a measure of the number of these interactions.

Knowing the integrated luminosity allows physicists to compare observations with theoretical predictions and simulations. For example, physicists can look for dark matter particles that escape collisions undetected by looking at the energies and momenta of all particles produced in a collision. If there is an imbalance, it could be caused by an undetected, potentially dark matter, particle carrying energy away. This is a powerful method of searching for a large class of new phenomena, but it has to take into account many effects, such as neutrinos produced in the collisions. Neutrinos also escape undetected and leave an energy imbalance, so in principle, they are indistinguishable from the new phenomena. To see if something unexpected has been produced, physicists have to look at the numbers.

If 11 000 events show an energy imbalance, and the simulations predict 10 000 events containing neutrinos, this could be significant. But if physicists only know luminosity with a precision of 10

There are also types of analyses that depend much less on absolute knowledge of the number of collisions. For example, in measurements of ratios of different particle decays, such as the recent LHCb measurement. Here, uncertainties in luminosity get cancelled out in the ratio calculations. Other searches for new particles look for peaks in mass distribution and so rely more on the shape of the observed distribution and less on the absolute number of events. But these also need to know the luminosity for any kind of interpretation of the results.

The experimental techniques to determine signal rates are mature enough, where the understanding of acceptances, detector biases, reconstruction efficiencies or background subtraction is at the subpercent level, so that the final precision of the physics measurement is dominated by the luminosity uncertainty [5].

Ultimately, the greater the precision of the luminosity measurement, the more physicists can understand their observations and delve into hidden corners beyond our current knowledge.

1.6 The Large Hadron Collider

The Large Hadron Collider (LHC) is the world's largest and most powerful particle accelerator. It first started up on 10 September 2008, and remains the latest addition to CERN's accelerator complex. The LHC consists of a 27-kilometre ring of superconducting magnets with a number of accelerating structures to boost the energy of the particles along the way.

Inside the accelerator, two high-energy particle beams travel at close to the speed of light before they are made to collide. The beams travel in opposite directions in separate beam pipes – two tubes kept at ultrahigh vacuum. They are guided around the accelerator ring by a strong magnetic field maintained by superconducting electromagnets. The electromagnets are built from coils of special electric cable that operates in a superconducting state, efficiently conducting electricity without resistance or loss of energy. This requires chilling the magnets to -271.3°C – a temperature colder than outer space.

Magnets of different varieties and sizes are used to direct the beams around the accelerator. These include 1232 dipole magnets, 15 metres in length, which bend the beams, and 392 quadrupole magnets, each 5–7 metres long, which focus the beams. Just prior to collision, another type of magnet is used to "squeeze" the particles closer together to increase the chances of collisions.

The bunches are previously accelerated by a chain of pre-accelerators. First, protons are produced by ionizing hydrogen and then are transferred to the Linear Accelerator 2 (LINAC2) where the protons are accelerated in bunches up to an energy of 50 MeV, and then the bunches pass through three circular accelerators: the Booster, the Proton Synchrotron (PS) and the Super Proton Synchrotron (SPS), giving an energy of 1.4 GeV, 26 GeV and 450 GeV, respectively. After these three preaccelerators, the bunches are finally circulating in opposite directions in the LHC ring, where they are further accelerated to reach energies up to 7 TeV (per bunch). This entire procedure defines a single LHC fill generally consisting of 10^{14} protons, grouped into bunches to form the proton beam.

All the controls for the accelerator, its services and technical infrastructure are housed under one roof at the CERN Control Centre. From here, the beams inside the LHC are made to collide at four locations around the accelerator ring, corresponding to the positions of four particle detectors: Compact Muon Solenoid (CMS) [6], ATLAS [7], ALICE [8] and LHCb [9]. CMS and ATLAS are for general-purpose detectors to investigate the largest range of SM and Beyond SM (BSM) physics. ALICE and LHCb have detectors specialized to study specific phenomena.

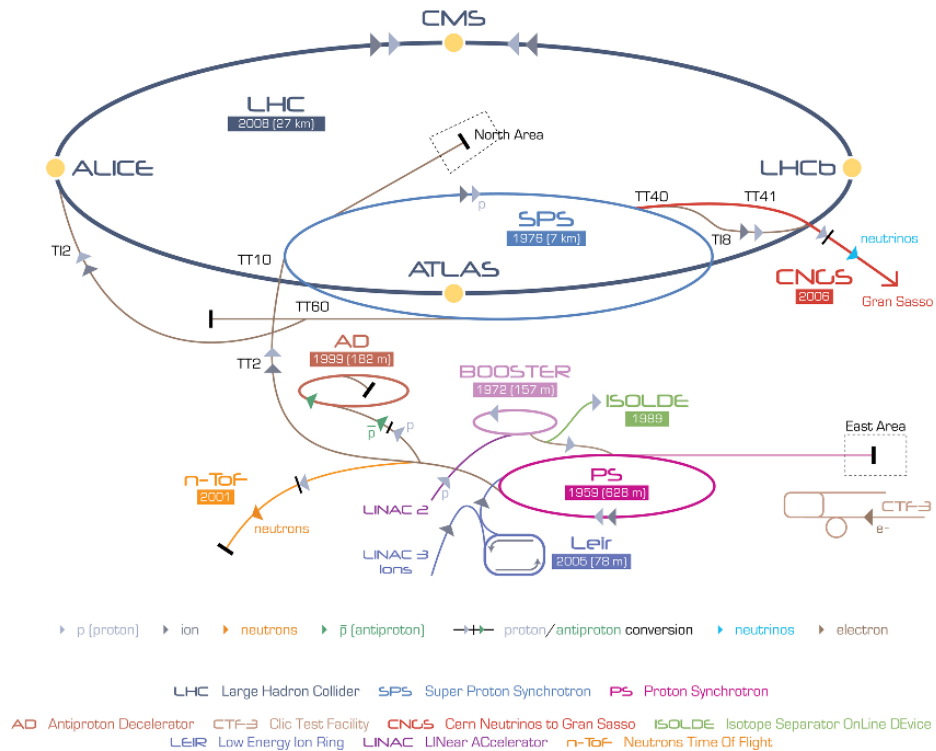


Fig. 1.3 Diagram of the LCH complex [10].

1.7 LHC Luminosity

Run 1 of the physics program at the Large Hadron Collider began in 2010 with pp collisions at a center of mass (CM) energy of 7 TeV. By the end of 2011, a data sample with integrated luminosity of $6fb^{-1}$ was collected by CMS. This Run finished at August 2012 with CM energy of 8 TeV with instantaneous peak luminosities approaching 0.77×10^{34} and an integrated luminosity of $25fb^{-1}$.

[11]

Run 2 was divided into two stages, the first was from 2015 to 2016 with proton-proton collisions at a center of mass energy (CM) of $\sqrt{s} = 13\text{TeV}$ in CMS detector, reaching a integrated luminosities of 2.2 and $36.3 fb^{-1}$ with a relative precision of 1.6% and 1.2%, respectively [12]. For the second part of Run 2 (2017-2018), the integrated luminosity is about $49.8fb^{-1}$ and $67.9fb^{-1}$ for 2017 and 2018 respectively, as can be seen in Fig. 1.4. The total systematic uncertainty in the calibration of luminosity measurement is 2.3% in 2017[13] and 2.5% in 2018 [14], but its precision remains to be improved.

Run 3 started in 2022 and is currently running, the main objective of this thesis project is to contribute to the improvement of the LHC luminosity precision calibration for this stage.

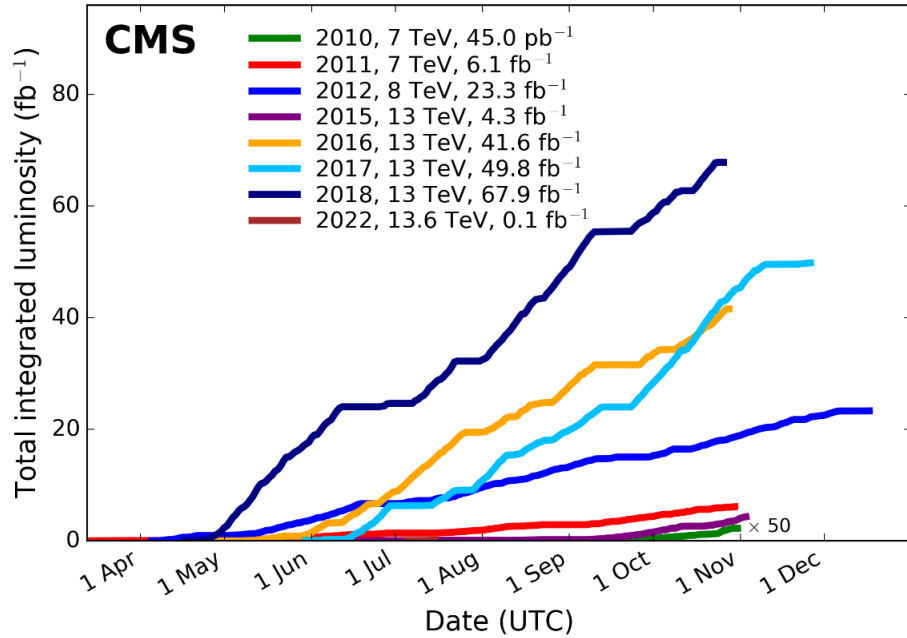


Fig. 1.4 Delivered luminosity versus time for Run-1 (2010-2012) and Run-2 (2015-2018); pp data only. Cumulative luminosity versus day delivered to CMS during stable beams for pp collisions at nominal center-of-mass energy. These plots use the best available offline calibrations for each year. For 2017 and 2018 the plots are based on [13] and [14], respectively [15].

Chapter 2

Experiment Description

2.1 The Compact Muon Solenoid

2.2 CMS Tracking System

2.2.1 Pixel Detector and Clustering

2.2.2 CMS Luminometers

Chapter 3

Luminosity Measurement and Calibration

3.1 Luminosity calibration: van der Meer method

Backgrounds

Chapter 4

Analysis and Results

4.1 2018 vdM scan program

4.2 Data analysis

4.3 Module selection

4.4 Background estimation

4.5 Corrections

Chapter 5

Summary and Outlook

References

- [1] Mark Thomson. *Modern Particle Physics*. Cambridge University Press, 2013. doi: 10.1017/CBO9781139525367.
- [2] David J Griffiths. *Introduction to elementary particles; 2nd rev. version*. Physics textbook. Wiley, New York, NY, 2008. URL <https://cds.cern.ch/record/111880>. <https://cds.cern.ch/record/111880>.
- [3] M.L. Mangano, Motivations and precision targets for an accurate luminosity determination at the LHC, *CERN-Proceedings-2011-011*, <https://cds.cern.ch/record/1347440>.
- [4] Stephen Myers and Herwig Schopper. *Particle Physics Reference Library Volume 3: Accelerators and Colliders*. 01 2020. doi: 10.1007/978-3-030-34245-6.
- [5] P. Grafström and W. Kozanecki. Luminosity determination at proton colliders. *Progress in Particle and Nuclear Physics*, 81:97–148, 2015. doi: <https://doi.org/10.1016/j.pnpnp.2014.11.002>.
- [6] CMS Collaboration. The CMS experiment at the CERN LHC. *Journal of Instrumentation*, 3(08):S08004–S08004, Aug 2008. doi: 10.1088/1748-0221/3/08/s08004.
- [7] ATLAS Collaboration. The ATLAS experiment at the CERN large hadron collider. *Journal of Instrumentation*, 3(08):S08003–S08003, Aug 2008. doi: 10.1088/1748-0221/3/08/s08003.
- [8] ALICE Collaboration. The ALICE experiment at the CERN LHC. *Journal of Instrumentation*, 3(08):S08002–S08002, Aug 2008. doi: 10.1088/1748-0221/3/08/s08002.
- [9] The LHCb Collaboration. The LHCb detector at the LHC. *Journal of Instrumentation*, 3(08):S08005–S08005, Aug 2008. doi: 10.1088/1748-0221/3/08/s08005.
- [10] Eva Halkiadakis. Introduction to the LHC Experiments. In *Theoretical Advanced Study Institute in Elementary Particle Physics: Physics of the Large and the Small*, pages 489–518, 2011. doi: 10.1142/9789814327183_0009.
- [11] Mike Lamont. Status of the LHC. *Journal of Physics: Conference Series*, 455: 012001, Aug 2013. doi: 10.1088/1742-6596/455/1/012001.
- [12] CMS Collaboration. Precision luminosity measurement in proton-proton collisions at $\sqrt{s} = 13$ tev in 2015 and 2016 at cms. *The European physical journal. C, Particles and fields*, 81:800, 01 2021. doi: 10.1140/epjc/s10052-021-09538-2.
- [13] CMS luminosity measurement for the 2017 data-taking period at $\sqrt{s} = 13$ TeV. Technical report, CERN, Geneva, 2018. URL <https://cds.cern.ch/record/2621960>.

-
- [14] CMS luminosity measurement for the 2018 data-taking period at $\sqrt{s} = 13$ TeV. Technical report, CERN, Geneva, 2019. URL <https://cds.cern.ch/record/2676164>.
- [15] CMSPublic Web. CMS Luminosity - Public Results. Delivered luminosity versus time for 2010-2012 and 2015-2018 (pp data only), 2022. URL <https://twiki.cern.ch/twiki/bin/view/CMSPublic/LumiPublicResults>. [Online; accessed September 23, 2022].